Real-Time Imaging of the Dynamics of Secretory Granules in Growth Cones

James R. Abney,*# C. Daniel Meliza,§ Bryan Cutler,* Mary Kingma,§ Janis E. Lochner,§ and Bethe A. Scalettar*

Departments of *Physics and §Chemistry, Lewis and Clark College, Portland, Oregon 97219, and #Kolisch, Hartwell, Dickinson, McCormack, and Heuser, P.C., Intellectual Property Attorneys, Portland, Oregon 97204 USA

ABSTRACT Secretory granules containing a hybrid protein consisting of the regulated secretory protein tissue plasminogen activator and an enhanced form of green fluorescent protein were tracked at high spatial resolution in growth cones of differentiated PC12 cells. Tracking shows that granules, unlike synaptic vesicles, generally are mobile in growth cones. Quantitative analysis of trajectories generated by granules revealed two dominant modes of motion: diffusive and directed. Diffusive motion was observed primarily in central and peripheral parts of growth cones, where most granules diffused two to four orders of magnitude more slowly than comparably sized spheres in dilute solution. Directed motion was observed primarily in proximal parts of growth cones, where a subset of granules underwent rapid, directed motion at average speeds comparable to those observed for granules in neurites. This high-resolution view of the dynamics of secretory granules in growth cones provides insight into granule organization and release at nerve terminals. In particular, the mobility of granules suggests that granules, unlike synaptic vesicles, are not tethered stably to cytoskeletal structures in nerve terminals. Moreover, the slow diffusive nature of this mobility suggests that secretory responses involving centrally distributed granules in growth cones will occur slowly, on a time scale of minutes or longer.

INTRODUCTION

Two fundamental regulated secretory processes occur at nerve terminals. First, proteins and neuropeptides are released from large secretory granules (also called secretory vesicles), facilitating a spectrum of biological processes that include extracellular matrix degradation, neuronal survival, and synaptic transmission (Thoenen, 1991; Hall, 1992; Patterson et al., 1992; Bean et al., 1994; Pittman and DiBenedetto, 1995; Burke et al., 1997; Haubensak et al., 1998; Lochner et al., 1998). Second, neurotransmitters are released from small synaptic vesicles, facilitating propagation of action potentials between pre- and postsynaptic cells (Hall, 1992; Bennett, 1997). Although much has been learned about both types of regulated secretion from nerve terminals, many of the underlying molecular events have yet to be elucidated.

Past studies of regulated secretion have revealed important similarities and differences in the behavior of secretory granules and synaptic vesicles in neuronal cells. Both organelles are present in nerve terminals, and both are secreted in response to stimuli that elevate intracellular calcium levels (Hall, 1992; Scheller and Hall, 1992; Bennett, 1997). However, granules are dispersed throughout terminals, and their release is induced by high-frequency electrical stimuli that may elevate calcium levels throughout the terminal (Hall, 1992; Scheller and Hall, 1992). In contrast, synaptic vesicles are concentrated in active zones, and their release is induced by lower-frequency stimuli that may induce changes in calcium levels, primarily near active zones (Augustine et al., 1991, 1992; Hall, 1992; Scheller and Hall, 1992; Smith et al., 1993). Both organelles appear to be present in nerve terminals in releasable and unreleasable pools; however, their release kinetics are markedly different (Ceccaldi et al., 1995; Burke et al., 1997). In the case of granules, the onset of most release after receipt of a stimulus is relatively slow, and the duration of most release is long (many minutes) (Bittner and Holz, 1992; Scheller and Hall, 1992; Burke et al., 1997). In contrast, in the case of synaptic vesicles, the onset of release is rapid, and the duration of release is short (milliseconds) (Llinás, 1982; Scheller and Hall, 1992).

Recently, the limited release of secretory granules from nerve terminals was linked to an apparent immobility of most cytoplasmic secretory granules (Burke et al., 1997), stimulating interest in granule dynamics in growth cones. However, the evidence for immobility was based on experiments with limited spatial resolution. Significantly, we recently developed a system that is well suited for high-resolution studies of granule dynamics in neuronal cells, including growth cones (Lochner et al., 1998). This system consists of neuroendocrine (PC12) cells that are transiently expressing a hybrid protein, tPA/GFP, consisting of the regulated secretory protein tissue plasminogen activator (tPA) with an enhanced form of green fluorescent protein (GFP) attached at the carboxy terminus (Cormack et al., 1996; Lochner et al., 1998). Importantly, tPA/GFP is efficiently targeted to regulated secretory granules, like endogenous tPA (Harrison et al., 1996; Parmer et al., 1997), and tPA/GFP is readily visualized using fluorescence micros-

Received for publication 19 May 1999 and in final form 11 August 1999.

Address reprint requests to Dr. Bethe A. Scalettar, Department of Physics, Lewis and Clark College, 0615 S.W. Palatine Hill Road, Portland, OR 97219-0532. Tel.: 503-768-7585; Fax: 503-768-7369; E-mail: bethe@lclark.edu.

0006-3495/99/11/2887/09 $2.00

copy in fixed and living cells (Lochner et al., 1998). Moreover, past studies of PC12 cells expressing tPA/GFP already have revealed novel features of granule dynamics along neurites and of the secretory behavior of tPA, including bidirectional transport of granules along neurites and regulated secretion of tPA from growth cones (Lochner et al., 1998).

Here we have used PC12 cells expressing tPA/GFP to characterize granule dynamics in growth cones. Specifically, we have tracked individual cytoplasmic secretory granules containing tPA/GFP in growth cones of living, differentiated PC12 cells at a spatial resolution of ~0.1 μm. By probing dynamics at high spatial resolution, we find that most granules in growth cones are (slowly) mobile over short distance scales, indicating that granules are not rigidly tethered to underlying cytoskeletal structures. We also find that granules in different regions of growth cones exhibit different dynamic behaviors, ranging from rapid and nonrandom motion in proximal parts of growth cones to very slow and random motion in peripheral parts of growth cones. Significantly, these features of granule dynamics provide further insight into factors that influence granule storage and release at nerve terminals.

MATERIALS AND METHODS

Cell culture and transient transfection

Stock PC12 cells (subclone GR-5) were grown on Primaria Plates (Becton Dickinson, Lincoln, NJ) at 37°C in a 5% CO_2/95% air incubator in Dulbecco's modified Eagle medium (DMEM) (Gibco BRL, Gaithersburg, MD) supplemented with 5% fetal calf serum and 5% horse serum. In preparation for fluorescence microscopy, cells were plated onto 25-mm-diameter round glass no. 1 coverslips (Fisher Scientific, Pittsburgh, PA) coated with a thin layer of dilute Matrigel (Collaborative Research, Waltham, MA). Cells were allowed to settle onto the coverslips and then were transferred into serum-free N_2 medium (Bottenstein and Sato, 1979) to induce the production of nerve growth factor (NGF) receptors. About 24 h after transfer into N_2 medium, the cells were induced to differentiate with 50 ng/ml NGF (Life Technologies, Gaithersburg, MD). About 72 h after addition of the NGF, the cells had extended long neurites that are similar to axons.

The gene for tPA/GFP was constructed with standard cloning techniques and was introduced into differentiated PC12 cells by lipid-based transient transfection techniques, as described previously (Lochner et al., 1998). Transfected PC12 cells were fixed or imaged live ~24 h posttransfection, at which time ~5% of the cells were expressing tPA/GFP.

Imaging

Images of the distribution and dynamics of secretory granules in transfected PC12 cells were collected on a DeltaVision wide-field optical-sectioning microscope system (Applied Precision, Issaquah, WA), as described previously (Lochner et al., 1998). All aspects of image collection were under automated control, which made it possible to rapidly collect time-lapse, multiwavelength, three-dimensional images.

For live (time-lapse) imaging, PC12 cells were mounted in Sykes-Moore chambers (Bellco Glass, Vineland, NJ) in imaging medium consisting of Dulbecco's glucose-supplemented phosphate-buffered saline (Gibco BRL) that was further supplemented with 2.5% fetal calf serum and 2.5% horse serum. The Sykes-Moore chamber was maintained at 31–37°C with a custom-heated holder.

The methodology of image acquisition depended on the type of image collected. Time-lapse images of granule dynamics in living PC12 cells were generated by taking images of the same focal plane every few seconds. These images were later deblurred using a constrained iterative deconvolution algorithm (Scalettar et al., 1996) to improve image clarity and to facilitate tracking of granules. Three-dimensional images of granule distribution in fixed PC12 cells were generated by optically sectioning cells in 0.2-μm focal increments (Hiraoka et al., 1991; Scalettar et al., 1996); three-dimensional images also were deblurred.

To ensure the reliability of dynamics data, granule dynamics in growth cones and granule transport along neurites were characterized simultaneously. In this way, it was possible to verify that cells were engaging in fast transport of granules along neurites throughout observation, indicating that the cells were healthy and undamaged by observation.

Data analysis

Dynamics was characterized by tracking positions of granules in growth cones as a function of time, where a growth cone was defined as that part of a neurite ending distal to the region where the neurite began to increase in width. This definition is consistent with the traditional view of a growth cone as a broad, flattened area at the end of a neurite (Alberts et al., 1994). To facilitate tracking, granule dynamics generally was studied in growth cones that were not too densely packed with fluorescent granules.

Granule dynamics was studied in different subregions of the growth cone: proximal, peripheral, and central. Granules generating a trajectory that crossed the region where the neurite ending began to increase in width were classified as proximal. Granules generating a trajectory that always remained within ~0.5 μm of the outline were classified as peripheral. The remaining granules were classified as central.

About 50 granules containing tPA/GFP were tracked visually in growth cones of six representative PC12 cells by playing time-lapse images of their positions as movies on an SGI workstation (Silicon Graphics, Mountain View, CA) running Priism image visualization software (Hiraoka et al., 1991). Granules were tracked as long as they could be unambiguously identified. During tracking, the Cartesian coordinates of the centers of granules were tabulated. Subsequently, these coordinates and the coordinates of the outline of the growth cone were entered into the program Igor Pro (WaveMetrics, Lake Oswego, OR). Granule coordinates then were converted into trajectories that were superimposed on the outline of the growth cone, creating a visual record of granule motion in growth cones.

Granule motion was characterized by studying the relationship between granule displacement and time. Specifically, we computed the mean squared displacement of granules as a function of time and fit the mean squared displacement to a model that includes the effects of "diffusive" and/or "directed" motion. Such a model can be expressed mathematically as follows (Berg, 1983; Saxton, 1994; Saxton and Jacobson, 1997):

$$\langle r^2(t)\rangle = 4Dt + v^2t^2 \qquad (1)$$

Here, r is displacement, t is time, D is the diffusion coefficient, and v is speed; brackets $\langle\ \rangle$ denote averaging, which was performed as described below. The first term on the right-hand side of Eq. 1 describes diffusion, and the second term describes directed motion. As shown by Eq. 1, diffusive motion is characterized by a linear relationship between mean squared displacement $\langle r^2\rangle$ and time, whereas directed motion is characterized by a linear relationship between *root* mean squared displacement $\langle r^2\rangle^{1/2}$ and time. The model underlying Eq. 1 assumes that the directed motion occurs with constant velocity, but the fitting procedure described below can handle slight variations in velocity by effectively averaging over them.

Granule motion was classified as diffusive and/or directed based on a visual examination of granule trajectories and on a least-squares fit to one or both terms of Eq. 1. To generate data that could be fit to Eq. 1, the mean squared displacement of tracked granules was computed for a series of

discrete time intervals, as follows:

$$\langle r^2(n\delta t)\rangle = \frac{1}{N-n+1}\sum_{i=0}^{N-n} |\vec{r}(i\delta t + n\delta t) - \vec{r}(i\delta t)|^2 \quad (2)$$

Here, N is the total number of steps in the trajectory, δt is the (constant) time interval associated with each step, and $n\delta t$ is the time interval over which displacement is averaged; vertical bars $\|$ denote magnitude. δt is determined by the speed of image acquisition and typically is 5–10 s. Similar methods have been shown to yield accurate results when diffusive motion is characterized using a limited set of particle coordinates (Saxton, 1997).

Generally, $\langle r^2(n\delta t)\rangle$ was computed for $n = 1$, 2, 3, and 4, and the results were fit to Eq. 1 using Igor Pro or Microsoft Excel (Microsoft, Redmond, WA). For virtually every granule, a fit of the mean squared displacement to Eq. 1 was overwhelmingly dominated by either the diffusive or directed term, indicating that the underlying motion was overwhelmingly dominated by either diffusive or directed motion. For this reason, data were reanalyzed by fitting $\langle r^2\rangle$ only to $4Dt$ for diffusive granules, and $\langle r^2\rangle^{1/2}$ only to vt for directed granules. The quality of each fit was assessed using 1) the coefficient of determination for the fit and 2) the ratio of the y intercept to the slope of the best-fit line. Fits were accepted only if the coefficient of determination was greater than 0.95 and the ratio of the y intercept to the slope was $<25\%$. Speed v was determined as the slope of the best-fit line for each linear $\langle r^2\rangle^{1/2}$ versus t plot, and the diffusion coefficient D was determined as one-fourth of the slope of the best-fit line for each linear $\langle r^2\rangle$ versus t plot.

Short-term directionality of diffusive granule movement in growth cones was quantified by comparing the relative proportion and average size of anterograde and retrograde steps. Anterograde and retrograde movement were easily distinguished, because all growth cones were oriented so that anterograde movement of a granule corresponded to a decrease in the y coordinate, and retrograde movement of a granule corresponded to an increase in the y coordinate. The relative proportions of anterograde and retrograde steps were determined by independently summing the number of anterograde and retrograde steps and dividing each sum by the total number of such steps. The average step size was determined by independently summing the y displacement of all anterograde and all retrograde steps and dividing each sum by the number of such steps.

RESULTS

Distribution

Fig. 1 shows a computationally deblurred optical section from a three-dimensional image of the distribution of tPA/GFP in a fixed PC12 cell. In this section, the neurite and growth cone are clearly in focus. The distribution pattern has three significant features. First, tPA/GFP is localized in large punctate structures, which we have shown to correspond to regulated secretory granules (Lochner et al., 1998). Second, granules containing tPA/GFP are found in neurites and growth cones, as well as the cell body. Finally, granules containing tPA/GFP are found throughout growth cones, except that they usually do not penetrate into filopodia, as determined by comparing phase and fluorescence images of growth cones (Lochner et al., 1998).

The density of fluorescent granules in neurites and growth cones varies with time and from cell to cell. In particular, the density of fluorescent granules tends to be lower at earlier times after transfection (Lochner et al., 1998). PC12 cells with lower densities of granules are better suited for granule tracking experiments, because granules may be distinguished more easily.

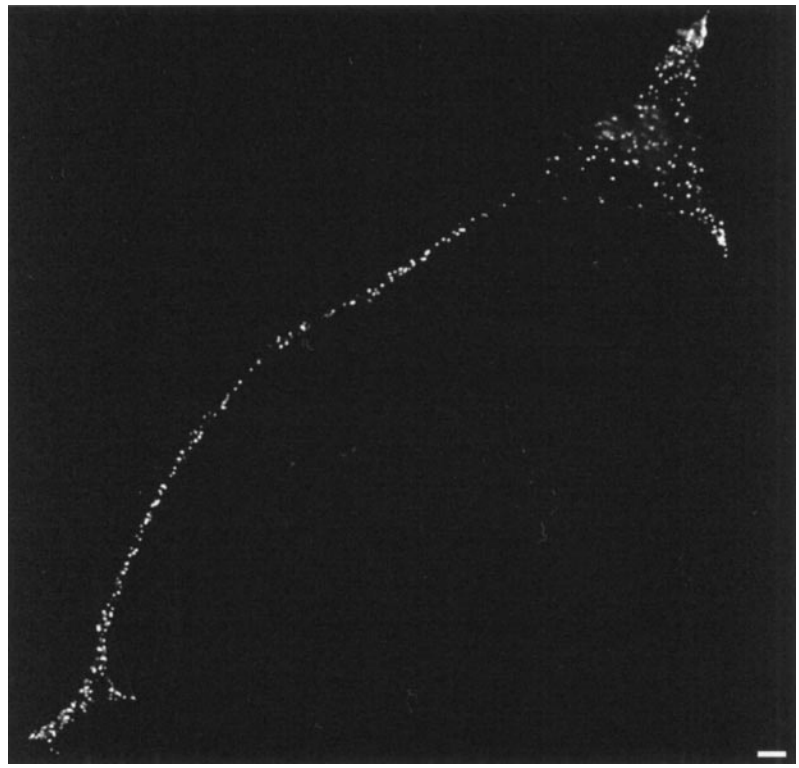

FIGURE 1 Deblurred image of a fixed PC12 cell expressing tPA/GFP. Bar, 4 μm.

Dynamics

Fig. 2, *A–C*, shows time-lapse, dual-color images of the distribution of granules containing tPA/GFP in the growth cones of three living, differentiated PC12 cells, in the absence of a stimulus to secrete (sample QuickTime movies corresponding to some of these images can be viewed at http://www.lclark.edu/~lochner/). Here, green indicates granule positions at an initial time, red indicates granule positions at a specified later time, and yellow indicates overlap of green and red. In Fig. 2, *A* and *B*, where the growth cones are relatively less fluorescent, granule overlap is lost gradually and substantially within ~50 s, showing that virtually all cytoplasmic granules in these growth cones are mobile over a time scale of <1 min. In contrast, in Fig. 2 *C*, where the growth cone is relatively more fluorescent, there is extensive granule overlap remaining after 50 s. This is especially true near the tip of this growth cone, where fluorescent granules are packed at very high density. Here, granule overlap could reflect granule immobility or exchange of one mobile granule for another. However, examination of movies generated from this growth cone revealed that most of the overlap is due to granule exchange arising from granule "jiggle," even in very dense areas. Apparently, most cytoplasmic granules in the interior of growth cones are not rigidly tethered to underlying cytoskeletal structures.

Significantly, there is some yellow remaining in Fig. 2, *A* and *B*, after 50 s. Some of this yellow again reflects exchange. However, some reflects very slow motion, preferentially corresponding to granules located near the periphery of growth cones and granules "trapped" in thin projections. This shows that peripheral granules tend to move more slowly than central granules, perhaps because they interact with the plasma membrane or structures associated with the plasma membrane.

Fig. 3, *A* and *B*, shows trajectories of 18 granules in the two (less fluorescent) growth cones in Fig. 2, *A* and *B*, superimposed on outlines of the growth cones. These 18 trajectories were selected for display because they illustrate the spectrum of dynamic behaviors exhibited by granules in the absence of a stimulus to secrete. These dynamic behaviors primarily include 1) rapid, substantially directed motion, and 2) slow, substantially random motion.

Granules *a–c* in Fig. 3 *A* provide examples of rapid, substantially directed granule motion. Rapid, directed motion is observed primarily in proximal parts of growth cones for granules entering (granule *a*) and exiting (granule *b*) the growth cone, and is occasionally observed in central parts of growth cones (granule *c*).

Granule *a* generated an especially complex trajectory. This granule first moved rapidly and nonrandomly into the growth cone and then began moving slowly and randomly after having penetrated into the growth cone interior. Thus this granule underwent a transformation in dynamic behavior from the rapid, directed motion characteristic of most granules in neurites to the slow, random motion characteristic of most granules in growth cones.

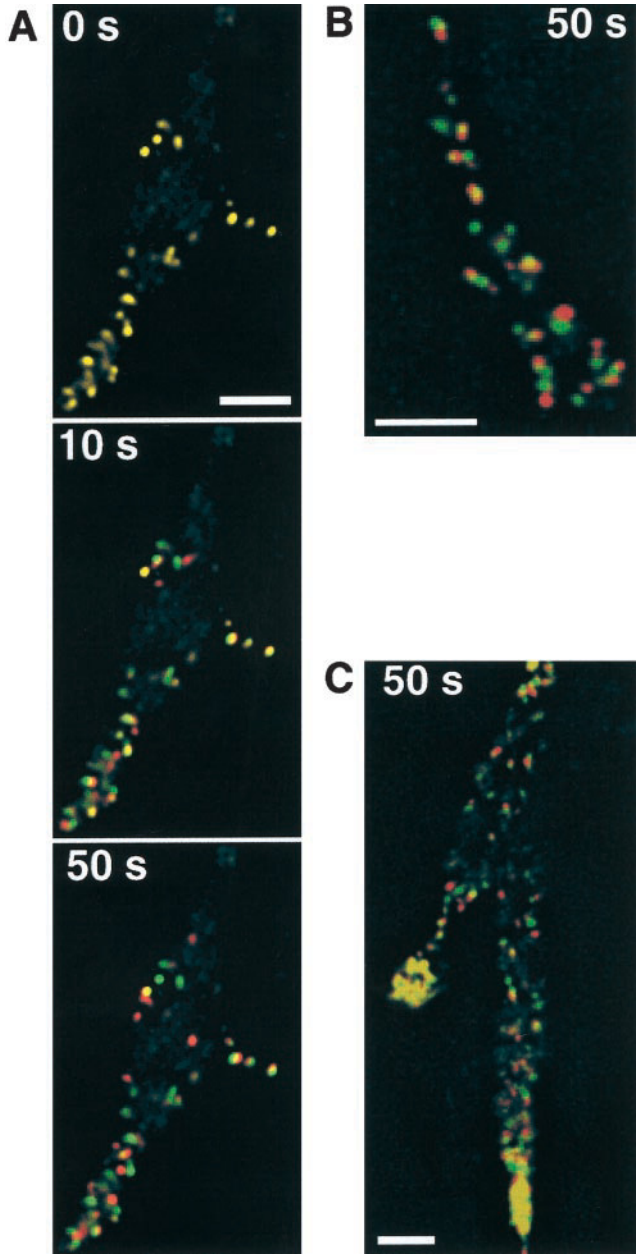

FIGURE 2 Dual-color images showing that the distribution of granules containing tPA/GFP in growth cones changes appreciably over the time scale of 50 s. In these images, green denotes granule positions at a fixed initial time, red denotes granule positions at the specified later time, and yellow denotes the overlap of green and red. For each growth cone, dual-color images were generated and analyzed for a series of at least six time points, with each time point separated from the last by 10 s; only a subset of these dual-color images is shown. After 50 s, overlap (*yellow*) in all three growth cones is associated mostly with partial motion or exchange, rather than true granule immobility. In all three panels, the distal part of the growth cone is oriented downward. In these images, lack of granule overlap arises from granule motion and not overall motion of the cell. This is clear from 1) the movies, 2) the fact that the overall outline of the cell did not shift, 3) the fact that granule movement was not correlated, and 4) the fact that a few granules basically did not move. Bar, 4 μm.

Granule *c* generated a trajectory that is somewhat unusually positioned, starting in a more central part of a growth cone. Generally, rapid directed motion occurs somewhat

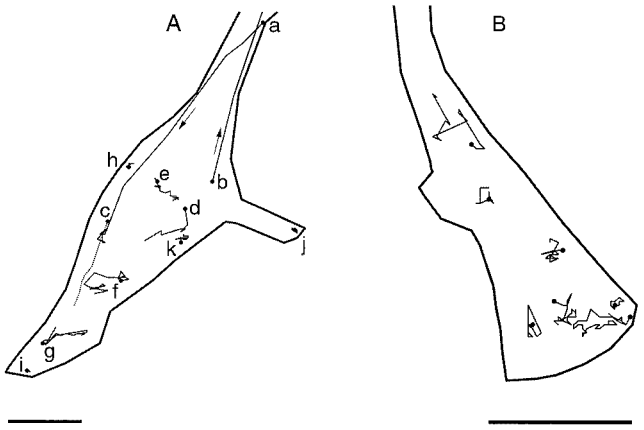

FIGURE 3 Trajectories of granules in the two (less fluorescent) growth cones in Fig. 2, *A* and *B*, superimposed on outlines of the growth cones. Starting granule positions are labeled with a filled circle. Arrows are used to indicate anterograde and retrograde directed motion. Not all of the trajectories shown were generated simultaneously. Bar, 4 μm.

closer to the proximal part of a growth cone, perhaps because granules in proximal parts of growth cones are more likely to be engaging in the fast directed motion that is exhibited by granules in neurites (Lochner et al., 1998). However, as granule *c* exemplifies, nonrandom, relatively rapid directed motion occasionally occurs in central parts of growth cones as well.

Granules *d–k* in Fig. 3 *A* provide examples of slow, substantially random granule motion. Slow, random motion is observed primarily in central and peripheral parts of the growth cone. Over short times, we observed a slight anterograde bias to this motion. Steps involving anterograde or retrograde motion were about evenly divided, but anterograde steps averaged 0.36 μm in length, whereas retrograde steps averaged 0.27 μm in length. Here, steps correspond to changes in granule positions during 10-s intervals. Over long times, motion clearly must be biased in the anterograde direction, because over long times fluorescent granules accumulate in the tips of growth cones (Lochner et al., 1998).

Virtually all granules were mobile. However, the rate and extent of mobility varied, depending in part on the location within the growth cone. In particular, randomly moving granules in central parts of growth cones generated longer trajectories than randomly moving granules in peripheral parts of growth cones, implying that granules in central parts are more mobile than granules in peripheral parts. This difference can be seen by comparing trajectories for granules *d–g* with trajectories for granules *h–j*.

The data in Fig. 3 reflect dynamics in the absence of a stimulus to secrete. We have also exposed living PC12 cells to classical secretagogues like carbachol that act as stimuli for regulated secretion (Harrison et al., 1996). In the presence of carbachol, it was possible to observe the integrated fluorescence intensity from growth cones as it fell to ~70% of its initial value over a time scale of ~20 min, indicating that a subset of granules containing tPA/GFP is slowly released from growth cones after stimulation (Lochner et al., 1998). However, it was difficult to detect changes in dynamics in the presence of carbachol, perhaps because only a small subset of granules participates in regulated secretory responses (Burke et al., 1997). Alternatively, it may have been difficult to detect changes because they were subtle, or because we were able to track granules only for times that were relatively short compared to the time scale of the regulated secretory response.

Fig. 4, *A* and *B*, characterizes the dynamics of individual granules quantitatively, showing representative plots of $\langle r^2\rangle^{1/2}$ versus t (Fig. 4 *A*) and $\langle r^2\rangle$ versus t (Fig. 4 *B*) that were derived from selected granule trajectories shown in Fig. 3.

Fig. 4 *A* shows that granules *a* and *c*, which appear in Fig. 3 to have undergone rapid and directed motion, generated trajectories that could be described quantitatively by the directed motion term v^2t^2 in Eq. 1, implying that $\langle r^2\rangle^{1/2}$ was proportional to t. Granule *a* generated the complex trajectory in Fig. 3 *A*, which has a fast, directed phase followed by a slow, random phase; the linear $\langle r^2\rangle^{1/2}$ versus t plot was generated using only data from the directed phase. Speeds v

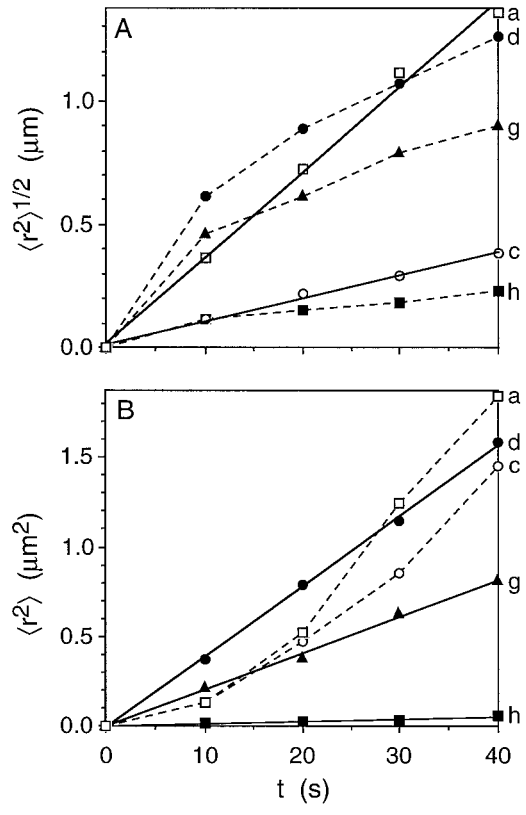

FIGURE 4 Representative plots of (*A*) $\langle r^2\rangle^{1/2}$ versus t and (*B*) $\langle r^2\rangle$ versus t deduced from the granule trajectories in Fig. 3. Letters next to the plots identify the trajectories in Fig. 3 from which the plots were derived. Some values were rescaled so that all plots could be displayed together conveniently. In *A*, values of $\langle r^2\rangle^{1/2}$ were divided by 10 for granules *a* and *c*. In *B*, values of $\langle r^2\rangle$ were divided by 100 and 10 for granules *a* and *c*, respectively.

computed from slopes of the $\langle r^2 \rangle^{1/2}$ versus t plots were 0.35 μm/s for granule a and 0.09 μm/s for granule c.

Fig. 4 B shows that granules d, g, and h, which appear to have undergone slow and random motion, generated trajectories that could be described quantitatively by the diffusive motion term $4Dt$ in Eq. 1, implying that $\langle r^2 \rangle$ was proportional to t. Diffusion coefficients D computed from slopes of the $\langle r^2 \rangle$ versus t plots were 9.9×10^{-11} cm^2/s for granule d, 5.1×10^{-11} cm^2/s for granule g, and 3.2×10^{-12} cm^2/s for granule h.

Most of the 50 or so measured trajectories were well fit by either the directed or diffusive motion terms of Eq. 1. As expected, trajectories that were well fit by one term generally were poorly fit by the other term, as shown by the dashed lines in Fig. 4, A and B.

A few trajectories were poorly fit by either or both terms of Eq. 1. Poor fits could reflect an inappropriateness of the model underlying Eq. 1. For example, some motion in cells has been ascribed to "anomalous" diffusion, in which $\langle r^2 \rangle$ is proportional to t^α, where α is between 0 and 1 (Scalettar and Abney, 1991; Saxton and Jacobson, 1997). However, poor fits also could reflect noise in the data. Most trajectories that were poorly fit by Eq. 1 corresponded to granules whose displacements were difficult to determine because they were small relative to the pixel size.

Fig. 5 is a histogram showing the distribution of diffusion coefficients obtained from all diffusing granules that we tracked. Diffusion coefficients were computed from slopes of linear $\langle r^2 \rangle$ versus t plots and were found to range between 2.1×10^{-12} cm^2/s and 5.4×10^{-10} cm^2/s, with a median of 3.9×10^{-11} cm^2/s. Heterogeneity in short-ranged granule diffusivities may reflect local heterogeneity in the cytoplasm of growth cones.

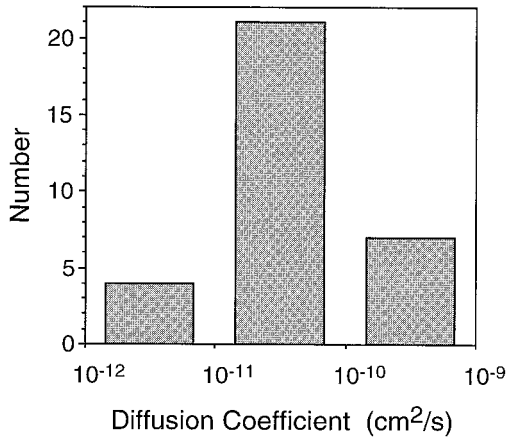

FIGURE 5 Distribution of diffusion coefficients obtained from tracking diffusing granules. Granules were classified as diffusing only if they generated $\langle r^2 \rangle$ versus t curves that were sufficiently linear, as described under Materials and Methods. Thus, only 32 granules are included in the histogram. Significantly, slowly mobile granules tended to fit a diffusion model poorly, because they moved small distances relative to our spatial resolution. Thus the histogram is somewhat biased toward mobile and faster moving granules; the median of the distribution is somewhat similarly biased.

DISCUSSION

The experiments described here were directed 1) at characterizing the dynamics of individual cytoplasmic secretory granules in growth cones of living neuronal cells at high spatial resolution, and 2) at relating the dynamics to current ideas about granule organization and release from nerve terminals.

Analysis of dynamics in growth cones

Subcellular structures can be mobile or immobile. Moreover, mobility can be diffusive, directed, or a combination of diffusive and directed (Scalettar and Abney, 1991; Saxton and Jacobson, 1997). Here we have demonstrated that virtually all cytoplasmic secretory granules in growth cones are mobile and that over short distance scales this mobility is primarily diffusive. However, diffusion of granules in growth cones is significantly slower than diffusion of comparably sized spherical particles in dilute solution. To demonstrate this, we calculated the diffusion coefficient of a spherical particle of radius 175 nm in dilute solution from the Stokes-Einstein relationship $D = k_B T/6\pi\eta r$ (Berg, 1983), where k_B is Boltzmann's constant, T is the absolute temperature ($\sim$300 K), η is the solution viscosity ($\sim 10^{-3}$ Pa s), and r is the radius of the sphere. A value of 175 nm is a reasonable upper bound for granule radii (Parsons et al., 1995), and thus the calculated diffusion coefficient will be an approximate lower bound for the diffusion coefficient of a granule in dilute solution. The calculated diffusion coefficient is $\sim 1.3 \times 10^{-8}$ cm^2/s, demonstrating that granule diffusion in the cytoplasm of growth cones is two to four orders of magnitude slower than in dilute solution. Such hindered mobility in cells and cell membranes has been observed previously for both exogenous and endogenous diffusors, ranging from small molecules to large cytoplasmic inclusions (Lang et al., 1986; Jacobson et al., 1987; Luby-Phelps et al., 1987; Alexander and Rieder, 1991; Kao et al., 1993).

There are several possible explanations for the hindered mobility of cytoplasmic granules (Kao et al., 1993). First, the growth cone is a congested environment, containing a high density of granules as well as many types of macromolecules, including microtubules and actin filaments (Forscher and Smith, 1988; Hirokawa et al., 1989). Such congestion could significantly hinder the movement of large structures like secretory granules, perhaps even leading to entrapment (Scalettar et al., 1988; Abney et al., 1989; Saxton, 1993). Second, granules, like synaptic vesicles (Hirokawa et al., 1989; Pieribone et al., 1995), may attach to cytoskeletal components in growth cones, either for long or short times. Such attachment also will hinder movement, leading to virtual immobilization if it is long lived and less severe inhibition of motion if it is transient (Kao et al., 1993). Of these possibilities, hindered motion of cytoplasmic granules in growth cones is most likely to reflect the effects of congestion or transient attachment to cytoskeletal

components, because granules move slowly but typically are not immobile.

Quantitative implications of slow granule diffusion

One potentially important consequence of slow granule diffusion is that cytoplasmic granules will require long times to traverse growth cones by diffusion. This is true even though growth cones are relatively small structures, with thicknesses typically of ~4 μm (Burke et al., 1997). To estimate these long times, we calculated an approximate time, t, required for a granule to explore distances on the order of the dimensions of a growth cone. The result is given by $\langle r^2 \rangle^{1/2} = (4Dt)^{1/2}$ (Berg, 1983), where t is in seconds and $\langle r^2 \rangle^{1/2} \approx 2$ μm (half the thickness of a growth cone). Solving for t gives 256 s, or >4 min; in obtaining this result, we have used the median diffusion coefficient obtained from tracking, 3.9×10^{-11} cm^2/s = 3.9×10^{-3} μm^2/s.

Comparison with previous studies of granule dynamics in growth cones

Granule dynamics in growth cones has not been studied extensively; moreover, somewhat disparate pictures have emerged from past work (Terakawa et al., 1993; Burke et al., 1997). The most quantitative and complete picture comes from fluorescence recovery after photobleaching (FRAP) studies of the mobility of cytoplasmically distributed secretory granules containing a preproatrial natriuretic factor/GFP hybrid in the growth cones of PC12 cells (Burke et al., 1997). Here we compare our tracking work with the FRAP work.

There are two important differences between tracking and FRAP that permit the techniques to yield complementary dynamic information (Saxton and Jacobson, 1997). First, tracking reveals the dynamics of individual molecules, whereas FRAP reveals the average dynamics of one or more subpopulations of molecules (such as mobile and immobile subpopulations). Second, the spatial resolution achieved with tracking usually is much better than the spatial resolution achieved with FRAP (Saxton and Jacobson, 1997); indeed, in the case of granules, the spatial resolutions achieved with tracking and FRAP were ~0.1 μm and ~2.0 μm, respectively (Burke et al., 1997).

FRAP, like tracking, shows that there are mobile granules in the cytoplasm of growth cones that typically move slowly. Specifically, in the FRAP experiments, it was assumed that mobile granules in growth cones diffuse, and based on this assumption a population-averaged diffusion coefficient of 4.9×10^{-11} cm^2/s was determined for the mobile granules. In the tracking experiments presented here, it was demonstrated explicitly that many granules in growth cones diffuse, and then diffusion coefficients ranging between 2.1×10^{-12} cm^2/s and 5.4×10^{-10} cm^2/s were determined for these granules. Significantly, the average D obtained from FRAP is quantitatively consistent with the median and range for D obtained from tracking. However, tracking shows that not all mobile granules in growth cones undergo diffusive motion; some undergo fast, directed motion reminiscent of granule motion along neurites (Lochner et al., 1998). Moreover, tracking reveals the heterogeneity in granule diffusivities.

FRAP, unlike tracking, suggests that there are many immobile granules in the cytoplasm of growth cones. Specifically, the FRAP experiments yielded large immobile fractions of ~70%. However, these experiments were unable to distinguish immobile granules and granules that were mobile but restricted in movement to distances less than 2 μm, because the spatial resolution of the experiments was limited (Burke et al., 1997). Significantly, high-resolution tracking experiments were able to distinguish these granules, demonstrating that essentially no granules in growth cones really are immobile. This kind of disparity in immobile fractions also is observed when tracking and FRAP are used to study the lateral mobility of proteins in biological membranes (Kusumi et al., 1993; Saxton and Jacobson, 1997).

Biological implications of dynamics

The tracking results bear on important issues surrounding 1) granule release from nerve terminals and 2) granule organization in nerve terminals, particularly the potential interaction of granules with the cytoskeleton and plasma membrane. We consider these issues in turn.

Granule release from nerve terminals is a complex process. For example, there is a fast phase of release occurring within ~1 min of stimulation and a slow phase of release occurring minutes after stimulation (Bittner and Holz, 1992; Burke et al., 1997). A very small fraction of granules is released rapidly, a larger (~30%) fraction of granules is released slowly, and a yet larger (~70%) fraction of granules is not released. These three groups of granules are known as the readily releasable, releasable, and reserve granule pools, respectively (Burke et al., 1997).

Recently it has been proposed that slow diffusion of mobile cytoplasmic granules determines the time scale of slow granule release from nerve terminals (Burke et al., 1997). In addition, it has been proposed that immobility (or possibly restricted mobility) of a large fraction of cytoplasmic granules limits the size of the secretory response (Burke et al., 1997). These proposals are based in large part on the FRAP data on granule mobility, as well as data suggesting that granules associated with slow release are distributed throughout growth cones and thus must move substantially during secretory responses (Burke et al., 1997; Lochner et al., 1998). We now consider how the tracking data impact these proposals.

Tracking demonstrates conclusively that most centrally distributed, cytoplasmic granules in growth cones diffuse

slowly in the absence of a stimulus to secrete and further suggests that changes in dynamics associated with stimulation are subtle. Thus the tracking data are consistent with the idea that slow granule diffusion can influence the time scale of slow release. Indeed, as demonstrated under Quantitative Implications of Slow Granule Diffusion, cytoplasmic granules will require times on the order of 4 min to diffuse distances on the order of the dimensions of a growth cone. Thus tracking predicts that slow secretory responses involving centrally distributed granules will last minimally for times on the order of 4 min after stimulation.

Tracking also demonstrates conclusively that most or all cytoplasmic granules in growth cones are mobile. Thus the tracking data are not consistent with the idea that granule immobility limits the size of the secretory response. However, restricted mobility or heterogeneity in mobility could influence the size of the response. For example, more slowly diffusing granules might not participate in the secretory response if they are too far from sites of exocytosis.

Finally, tracking demonstrates that a small population of peripherally distributed granules diffuses very slowly. Thus the tracking data suggest that some peripheral granules may interact with the plasma membrane or structures associated with the plasma membrane, leading to slowing. Interestingly, recent studies using evanescent-wave microscopy have also revealed a population of membrane-apposed secretory granules in chromaffin cells that diffuses very slowly ($D \approx 10^{-12}$ cm^2/s) (Steyer et al., 1997; Oheim et al., 1998, 1999; Steyer and Almers, 1999). Given the similarity in their behavior, the nearly immobile granule populations in chromaffin cells and growth cones of PC12 cells may arise by similar mechanisms.

Comparison of the dynamics of secretory granules and synaptic vesicles

It is interesting and instructive to compare the mobility of secretory granules and synaptic vesicles in growth cones. The mobility of synaptic vesicles has been studied recently in several systems by the use of FRAP (Henkel et al., 1996; Kraszewski et al., 1996). These studies have shown that synaptic vesicles in terminals, unlike granules, generally appear to be completely immobile before exocytosis. The apparent difference in mobility between synaptic vesicles and granules may reflect the fact that synaptic vesicles, unlike granules, are clustered near active zones before exocytosis (Kandel, 1991). Perhaps more importantly, synaptic vesicles, unlike granules, appear to be tethered stably to cytoskeletal structures through an interaction mediated by synapsins (Hirokawa et al., 1989; Kandel, 1991; Ceccaldi et al., 1995; Pieribone et al., 1995).

Comparison of the dynamics of granules in growth cones and neurites

The dynamics of secretory granules in growth cones and neurites are markedly different. As shown here, most cytoplasmic granules in growth cones diffuse slowly, and only a small percentage move unidirectionally. In contrast, most granules in neurites move nondiffusively and rapidly ($\langle v \rangle \approx 0.5$ μm/s), and ~85% move unidirectionally (Lochner et al., 1998). Thus, after entering the confined volume of the growth cone, granules undergo a change in motion from primarily rapid and nonrandom to primarily slow and random.

The differences in dynamic behavior exhibited by granules in neurites and growth cones can be rationalized to some degree. Neurites serve to transport granules over long distances (Hirokawa, 1993). Thus granule motion along neurites needs to be rapid and directed, facilitating long-distance transport (Kreis et al., 1989; Hirokawa, 1993; Lochner et al., 1998). In contrast, growth cones serve as preferential sites of granule storage and secretion (Rivas and Moore, 1989; Harrison et al., 1996; Gutierrez et al., 1998; Lochner et al., 1998). Thus granule motion in growth cones does not need to be rapid and directed, at least in the absence of a stimulus to secrete.

The molecular origins of the differences in dynamic behavior in neurites and growth cones are not completely clear, but they may reflect changes in interactions between granules and microtubules. Granules and their associated motor proteins appear to translocate actively along microtubules during transport along neurites, ensuring that nonrandom motion is the dominant dynamic mode (Kreis et al., 1989; Lochner et al., 1998). In contrast, granules and their associated motors may largely detach from microtubules at some point after entering the growth cone, permitting diffusion to become the dominant dynamic mode. Alternatively, granules in growth cones, like constitutively secreted vesicles in Vero cell bodies, may maintain some interaction with microtubules while moving randomly (Wacker et al., 1997).

This work was supported by National Science Foundation grant BIR-9510226 (to JEL and BAS) and Research Corporation grant CC3819 (to BAS).

REFERENCES

Abney, J. R., B. A. Scalettar, and J. C. Owicki. 1989. Self diffusion of interacting membrane proteins. *Biophys. J.* 55:817–833.

Alberts, B., D. Bray, J. Lewis, M. Raff, K. Roberts, and J. D. Watson. 1994. Molecular Biology of the Cell, 3rd Ed. Garland, New York.

Alexander, S. P., and C. L. Rieder. 1991. Chromosome motion during attachment to the vertebrate spindle: initial saltatory-like behavior of chromosomes and quantitative analysis of force production by nascent kinetochore fibers. *J. Cell Biol.* 113:805–815.

Augustine, G. J., E. M. Adler, and M. P. Charlton. 1991. The calcium signal for transmitter secretion from presynaptic nerve terminals. *Ann. N. Y. Acad. Sci.* 635:365–381.

Augustine, G. J., E. M. Adler, M. P. Charlton, M. Hans, D. Swandulla, and K. Zipser. 1992. Presynaptic calcium signals during neurotransmitter release: detection with fluorescent indicators and other calcium chelators. *J. Physiol. (Paris).* 86:129–134.

Bean, A. J., X. Zhang, and T. Hökfelt. 1994. Peptide secretion: what do we know? *FASEB J.* 8:630–638.

Bennett, M. K. 1997. Ca^{2+} and the regulation of neurotransmitter secretion. *Curr. Opin. Neurobiol.* 7:316–322.

Berg, H. 1983. Random Walks in Biology. Princeton University Press, Princeton, NJ.

Bittner, M. A., and R. W. Holz. 1992. Kinetic analysis of secretion from permeabilized adrenal chromaffin cells reveals distinct components. *J. Biol. Chem.* 267:16219–16225.

Bottenstein, J. E., and G. H. Sato. 1979. Growth of a rat neuroblastoma cell line in serum-free supplemented medium. *Proc. Natl. Acad. Sci. USA.* 76:514–517.

Burke, N. V., W. Han, D. Li, K. Takimoto, S. C. Watkins, and E. S. Levitan. 1997. Neuronal peptide release is limited by secretory granule mobility. *Neuron.* 19:1095–1102.

Ceccaldi, P.-E., F. Grohovaz, F. Benfenati, E. Chieregatti, P. Greengard, and F. Valtorta. 1995. Dephosphorylated synapsin I anchors synaptic vesicles to actin cytoskeleton: an analysis by videomicroscopy. *J. Cell Biol.* 128:905–912.

Cormack, B. P., R. H. Valdivia, and S. Falkow. 1996. FACS-optimized mutants of the green fluorescent protein (GFP). *Gene.* 173:33–38.

Forscher, P., and S. J. Smith. 1988. Actions of cytochalasins on the organization of actin filaments and microtubules in a neuronal growth cone. *J. Cell Biol.* 107:1505–1516.

Gutierrez, L. M., A. Gil, and S. Viniegra. 1998. Preferential localization of exocytotic active zones in the terminals of neurite-emitting chromaffin cells. *Eur. J. Cell Biol.* 76:274–278.

Hall, Z. W. 1992. The nerve terminal. *In* An Introduction to Molecular Neurobiology. Z. W. Hall, editor. Sinauer Associates, Sunderland, MA.

Harrison, T. M., M. A. J. Chidgey, and S. Uff. 1996. Novel markers for constitutive secretion used to show that tissue plasminogen activator is sorted to the regulated pathway in transfected PC12 cells. *Cell Biol. Int.* 20:293–300.

Haubensak, W., F. Narz, R. Heumann, and V. Lessmann. 1998. BDNF-GFP containing secretory granules are localized in the vicinity of synaptic junctions of cultured cortical neurons. *J. Cell Sci.* 111:1483–1493.

Henkel, A. W., L. L. Simpson, R. M. A. P. Ridge, and W. J. Betz. 1996. Synaptic vesicle movements monitored by fluorescence recovery after photobleaching in nerve terminals stained with FM1–43. *J. Neurosci.* 16:3960–3967.

Hiraoka, Y., J. R. Swedlow, M. R. Paddy, D. A. Agard, and J. W. Sedat. 1991. Three-dimensional multiple-wavelength fluorescence microscopy for the structural analysis of biological phenomena. *Semin. Cell Biol.* 2:153–165.

Hirokawa, N. 1993. Axonal transport and the cytoskeleton. *Curr. Opin. Neurobiol.* 3:724–731.

Hirokawa, N., K. Sobue, K. Kanda, A. Harada, and H. Yorifuji. 1989. The cytoskeletal architecture of the presynaptic terminal and molecular structure of synapsin 1. *J. Cell Biol.* 108:111–126.

Jacobson, K., A. Ishihara, and R. Inman. 1987. Lateral diffusion of proteins in membranes. *Annu. Rev. Physiol.* 49:163–175.

Kandel, E. R. 1991. Transmitter release. *In* Principles of Neural Science, 3rd Ed. E. R. Kandel, J. H. Schwartz, and T. M. Jessell, editors. Appleton and Lange, Norwalk, CT.

Kao, H. P., J. R. Abney, and A. S. Verkman. 1993. Determinants of the translational mobility of a small solute in cell cytoplasm. *J. Cell Biol.* 120:175–184.

Kraszewski, K., L. Daniell, O. Mundigl, and P. De Camilli. 1996. Mobility of synaptic vesicles in nerve endings monitored by recovery from photobleaching of synaptic vesicle-associated fluorescence. *J. Neurosci.* 16:5905–5913.

Kreis, T. E., R. Matteoni, M. Hollinshead, and J. Tooze. 1989. Secretory granules and endosomes show saltatory movement biased to the anterograde and retrograde directions, respectively, along microtubules in AtT20 cells. *Eur. J. Cell Biol.* 49:128–139.

Kusumi, A., Y. Sako, and M. Yamamoto. 1993. Confined lateral diffusion of membrane receptors as studied by single particle tracking (nanovid microscopy). Effects of calcium-induced differentiation in cultured epithelial cells. *Biophys. J.* 65:2021–2040.

Lang, I., M. Scholz, and R. Peters. 1986. Molecular mobility and nucleocytoplasmic flux in hepatoma cells. *J. Cell Biol.* 102:1183–1190.

Llinás, R. R. 1982. Calcium in synaptic transmission. *Sci. Am.* 247:56–65.

Lochner, J. E., M. Kingma, S. Kuhn, C. D. Meliza, B. Cutler, and B. A. Scalettar. 1998. Real-time imaging of the axonal transport of granules containing a tissue plasminogen activator/green fluorescent protein hybrid. *Mol. Biol. Cell.* 9:2463–2476.

Luby-Phelps, K., P. E. Castle, D. L. Taylor, and F. Lanni. 1987. Hindered diffusion of inert tracer particles in the cytoplasm of mouse 3T3 cells. *Proc. Natl. Acad. Sci. USA.* 84:4910–4913.

Oheim, M., D. Loerke, W. Stühmer, and R. H. Chow. 1998. The last few milliseconds in the life of a secretory granule. *Eur. Biophys. J.* 27:83–98.

Oheim, M., D. Loerke, W. Stühmer, and R. H. Chow. 1999. Multiple stimulation-dependent processes regulate the size of the releasable pool of vesicles. *Eur. Biophys. J.* 28:91–101.

Parmer, R. J., M. Mahata, S. Mahata, M. T. Sebald, D. T. O'Connor, and L. A. Miles. 1997. Tissue plasminogen activator (t-PA) is targeted to the regulated secretory pathway. Catecholamine storage vesicles as a reservoir for the rapid release of t-PA. *J. Biol. Chem.* 272:1976–1982.

Parsons, T. D., J. R. Coorssen, H. Horstmann, and W. Almers. 1995. Docked granules, the exocytic burst, and the need for ATP hydrolysis in endocrine cells. *Neuron.* 15:1085–1096.

Patterson, S. L., L. M. Grover, P. A. Schwartzkroin, and M. Bothwell. 1992. Neurotrophin expression in rat hippocampal slices: a stimulus paradigm inducing LTP in CA1 evokes increases in BDNF and NT-3 mRNAs. *Neuron.* 9:1081–1088.

Pieribone, V. A., O. Shupliakov, L. Brodin, S. Hilfiker-Rothenfluh, A. J. Czernik, and P. Greengard. 1995. Distinct pools of synaptic vesicles in neurotransmitter release. *Nature.* 375:493–497.

Pittman, R. N., and A. J. DiBenedetto. 1995. PC12 cells overexpressing tissue plasminogen activator regenerate neurites to a greater extent and migrate faster than control cells in complex extracellular matrix. *J. Neurochem.* 64:566–575.

Rivas, R. J., and H.-P. H. Moore. 1989. Spatial segregation of the regulated and constitutive secretory pathways. *J. Cell Biol.* 109:51–60.

Saxton, M. J. 1993. Lateral diffusion in an archipelago. Dependence on tracer size. *Biophys. J.* 64:1053–1062.

Saxton, M. J. 1994. Single-particle tracking: models of directed transport. *Biophys. J.* 67:2110–2119.

Saxton, M. J. 1997. Single-particle tracking: the distribution of diffusion coefficients. *Biophys. J.* 72:1744–1753.

Saxton, M. J., and K. Jacobson. 1997. Single-particle tracking: applications to membrane dynamics. *Annu. Rev. Biophys. Biomol. Struct.* 26: 373–399.

Scalettar, B. A., and J. R. Abney. 1991. Molecular crowding and protein diffusion in biological membranes. *Comm. Mol. Cell. Biophys.* 7:79–107.

Scalettar, B. A., J. R. Abney, and J. C. Owicki. 1988. Theoretical comparison of the self diffusion and mutual diffusion of interacting membrane proteins. *Proc. Natl. Acad. Sci. USA.* 85:6726–6730.

Scalettar, B. A., J. R. Swedlow, J. W. Sedat, and D. A. Agard. 1996. Dispersion, aberration and deconvolution in multi-wavelength fluorescence images. *J. Microsc.* 182:50–60.

Scheller, R. H., and Z. W. Hall. 1992. Chemical messengers at synapses. *In* An Introduction to Molecular Neurobiology. Z. W. Hall, editor. Sinauer Associates, Sunderland, MA.

Smith, S. J., J. Buchanan, L. R. Osses, M. P. Charlton, and G. J. Augustine. 1993. The spatial distribution of calcium signals in squid presynaptic terminals. *J. Physiol. (Lond.).* 472:573–593.

Steyer, J. A., and W. Almers. 1999. Tracking single secretory granules in live chromaffin cells by evanescent-field fluorescence microscopy. *Biophys. J.* 76:2262–2271.

Steyer, J. A., H. Horstmann, and W. Almers. 1997. Transport, docking and exocytosis of single secretory granules in live chromaffin cells. *Nature.* 388:474–478.

Terakawa, S., S. Manivannan, and K. Kumakura. 1993. Evidence against the swelling hypothesis for initiation of exocytosis in terminals of chromaffin cell processes. *J. Physiol. (Paris).* 87:209–213.

Thoenen, H. 1991. The changing scene of neurotrophic factors. *Trends Neurosci.* 14:165–170.

Wacker, I., C. Kaether, A. Kromer, A. Migala, W. Almers, and H.-H. Gerdes. 1997. Microtubule-dependent transport of secretory vesicles visualized in real time with a GFP-tagged secretory protein. *J. Cell Sci.* 110:1453–1463.